Energy Conversion and Management 151 (2017) 123–135

Contents lists available at ScienceDirect

Energy Conversion and Management

journal homepage: www.elsevier.com/locate/enconman

Investigation on efficiency improvement of a Kalina cycle by sliding condensation pressure method

Enhua Wang[a,b], Zhibin Yu[b,*], Fujun Zhang[a]

[a] School of Mechanical Engineering, Beijing Institute of Technology, Beijing 100081, China
[b] School of Engineering, University of Glasgow, Glasgow G12 8QQ, UK

ARTICLE INFO

Keywords:
Kalina cycle
Sliding condensation pressure
Composition tuning
Ambient temperature match
Ammonia-water mixture

ABSTRACT

Conventional Kalina cycle-based geothermal power plants are designed with a fixed working point determined by the local maximum ambient temperature during the year. A previous study indicated that the plant's annual average thermal efficiency would be improved if the ammonia mass fraction of the Kalina cycle could be tuned to adapt to the ambient conditions. In this paper, another sliding condensation pressure method is investigated. A theoretical model is set up and then a numerical program is developed to analyze the cycle performance. The condensation pressure adjustment in accordance to the changing ambient temperature has been numerically demonstrated under various ammonia-water mixture concentrations. The results indicate that the Kalina cycle using sliding condensation pressure method can achieve much better annual average thermal efficiency than a conventional Kalina cycle through matching the cycle with the changing ambient temperature via controlling condensation pressure. Furthermore, the sliding condensation pressure method is compared with the composition tuning method. The results show that the annual average efficiency improvement of the sliding condensation pressure method is higher than that of the composition tuning method.

1. Introduction

Geothermal energy has many advantages such as weatherproof, base-load power, high stability and reliability, less land usage, and less ecological effect [1]. With the progress of technology, power generation from low-temperature geothermal energy becomes economically attractive [2]. An annual average increment of 350 MW/year in the world has been achieved in the five-year term 2010–2015, mainly from the increase in medium-low temperature projects through binary plants [3].

The Kalina cycle uses a zeotropic mixture as the working fluid (normally ammonia-water) and can be applied for low-temperature geothermal power generation [4,5]. Hua et al. designed a triple-pressure ammonia-water power cycle and the results showed that the power recovery efficiency was about 16.6% higher than that of a steam Rankine cycle [6]. Pradeep Varma and Srinivas compared the thermodynamic performances of the Kalina cycle with organic Rankine cycle and organic flash cycle [7]. Fallah used an advanced exergy method to analyze a Kalina cycle system 11 (denoted as KCS-11 hereafter) [8]. Ma et al. compared three advanced absorption power cycles with KCS-11 system in terms of power output, energy and exergy efficiencies for low-temperature heat sources [9].

Among various Kalina cycle systems, KCS-34 is suitable for low-temperature heat sources [10]. A geothermal power plant was built in Husavik, Iceland in 2000 based on the KCS-34 Kalina cycle [11]. Saffari et al. carried out a thermodynamic analysis for the geothermal Kalina cycle employed in Husavik power plant using an artificial bee colony algorithm and the optimum thermal efficiency could achieve 20.36% [12]. Arslan investigated the performance of the KCS-34 cycle system using an artificial neural network and life cycle cost analysis and found that the most profitable ammonia mass fraction ranges from 80% to 90% [13].

In 2007, Lengert altered the position of the recuperator of the KCS-34 Kalina cycle and patented a new power cycle, i.e., the so-called KSG-1 Kalina cycle [14]. Mergner and Weimer compared the thermodynamic performances between the KSG-1 and KCS-34 Kalina cycles for geothermal power generation and the KSG-1 Kalina cycle achieved a slightly higher efficiency than the KCS-34 [15].

Various methods have been proposed to further improve the performance of Kalina cycle when the environmental conditions vary. Ibrahim and Kovach controlled the temperature of the ammonia-water mixture in the separator so that the ammonia mass fraction at the expander inlet could be adjusted [16]. Nguyen et al. studied a Kalina split-cycle concept that had a varying ammonia concentration during the

* Corresponding author.
E-mail address: Zhibin.Yu@glasgow.ac.uk (Z. Yu).

http://dx.doi.org/10.1016/j.enconman.2017.08.078
Received 19 May 2017; Received in revised form 17 August 2017; Accepted 27 August 2017

Nomenclature

$\dot{E}$	exergy (kJ)
h	enthalpy (kJ/kg)
$\dot{I}$	exergy destruction rate (kW)
$\dot{m}$	mass flow rate (kg/s)
P	pressure (MPa)
$\dot{Q}$	heat quantity (kW)
s	entropy (kJ/kg K)
T	temperature (K)
$\dot{W}$	power (kW)
x	ammonia mass fraction

Greek letters

α	improvement of net power output
β	improvement of heat transfer from the heat source
γ	improvement of thermal efficiency
η	efficiency

Subscript

0, a	ambient condition
b	basic solution
c	condenser
e	evaporator
ex	exergy efficiency
f	fan
m	mixer
n	net
p	pump
re	recuperator
s	separator
t	turbine
th	thermal efficiency
v	expansion valve

preheating and evaporation stages [17]. Recently, Mlcak and Mirolli invented a method to adjust the ammonia mass fraction according to the cooling source temperature to improve cycle efficiency [18]. Wang and Yu evaluated the efficiency improvement of this composition tuning method and found that the average thermal efficiency could be enhanced significantly [19].

The above investigations indicate that the performance of the Kalina cycle can be improved via adjusting the ammonia mass fraction. On the other hand, the sliding pressure control method is often used for steam Rankine cycles to improve the system efficiency [20–22]. In this method, when the Rankine cycle system operates on part-load conditions especially at low-load working points, the operation pressure at the inlet of the high-pressure turbine decreases as the load drops. To adapt to the variable geothermal fluid mass flow rate and temperature, Hu et al. performed an off-design performance analysis of an organic Rankine cycle system using three different control strategies including sliding pressure control [23]. Normally, sliding pressure control is used to fulfil the varying demand in load by changing evaporation pressure. Usman et al. experimentally investigated the performance of an organic Rankine cycle using sliding pressure control approach [24]. Compared with the organic Rankine cycle using a pure working fluid, the Kalina cycle uses a zeotropic working fluid such as an ammonia-water mixture and has an additional degree of freedom in terms of the ammonia mass fraction. Modi et al. [25] and Li et al. [26] investigated the off-design performances of the Kalina cycle using sliding pressure control. However, no investigation was reported to evaluate the efficiency improvement of the Kalina cycle using sliding condensation pressure method when the ambient temperature varies. Furthermore, it is meaningful to compare the efficiency improvement of the Kalina cycle between using sliding condensation pressure method and the composition tuning method.

The ambient temperature normally fluctuates with days and seasons. When the ambient temperature varies, the corresponding temperature at the outlet of the air-cooled condenser also changes if the pinch-point temperature difference inside the condenser is constant. Because the ammonia-water zeotropic mixture is in a saturated liquid

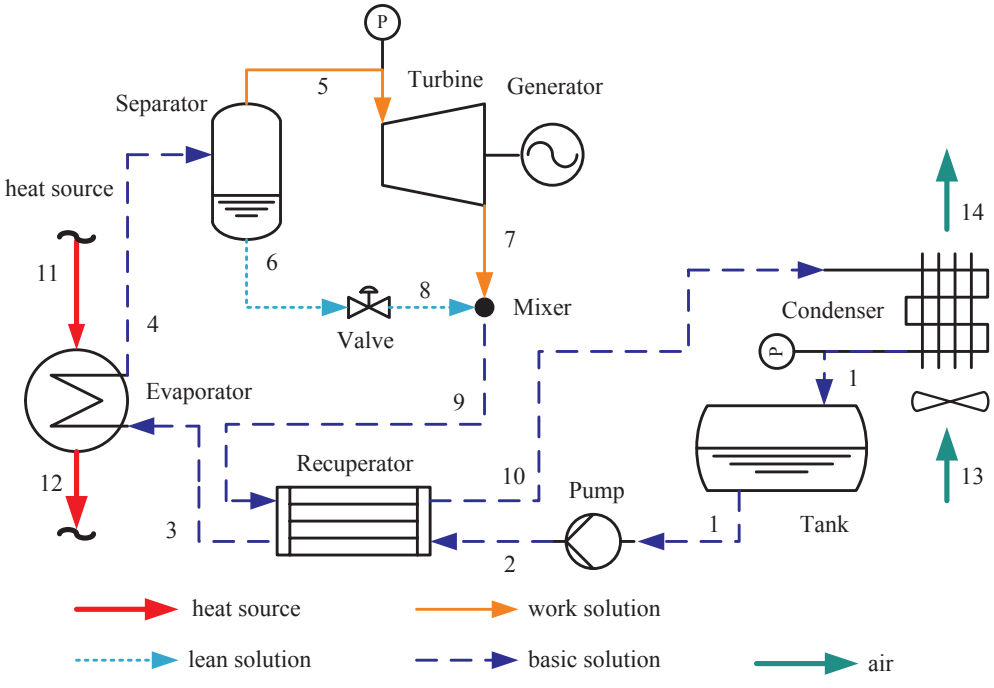

Fig. 1. Schematic of KSG-1 Kalina cycle for low-temperature geothermal power generation.

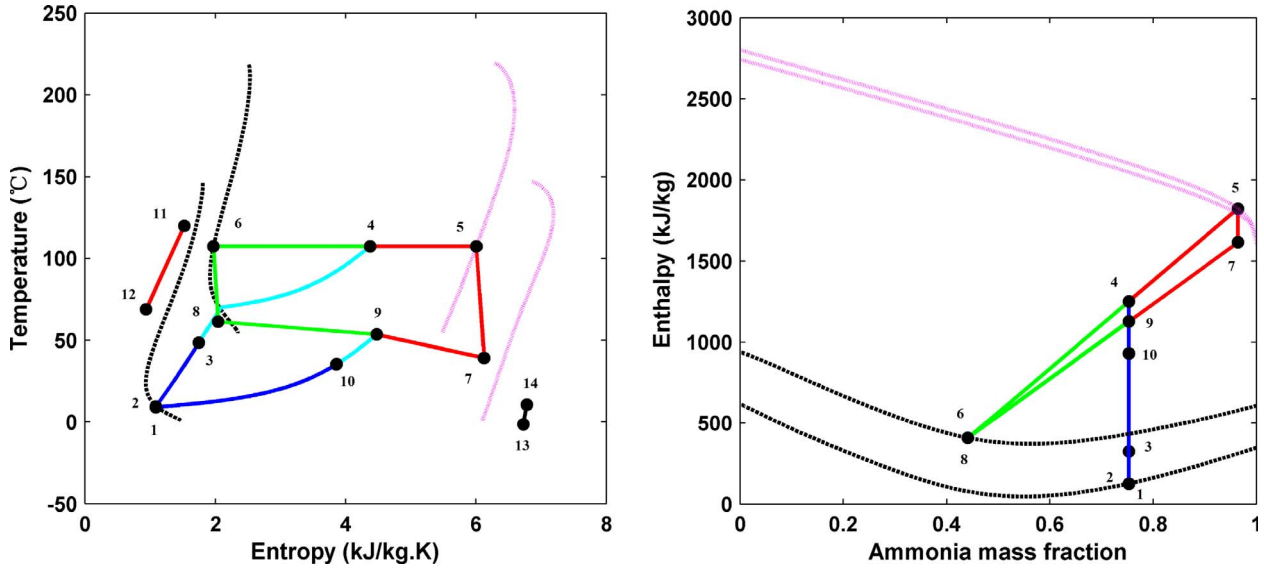

Fig. 2. Working processes of KSG-1 Kalina cycle: (a) T-s diagram, (b) h-x diagram.

state, which is located on the bubble line at this moment, the condensation pressure will also change with the ambient temperature for a fixed ammonia mass fraction. Based on this principle, the sliding condensation pressure method will regulate the condensation pressure to keep the working fluid temperature at the outlet of the condenser close enough to the ambient temperature. In order to address this problem, this paper theoretically investigates the efficiency improvement of the KSG-1 Kalina cycle system using the sliding condensation pressure method and then the results are compared with that of the composition tuning method. The problem of whether the system can remain in the high-efficiency regions by adjusting the condensation pressure as the ambient temperature varies is clarified. Matching the condensation pressure with the ambient temperature in a manner of sliding condensation pressure, the improvement of the annual average thermal efficiency is evaluated compared with the conventional Kalina cycle. Furthermore, the efficiency improvement of the sliding condensation pressure method is compared with that of the composition tuning method.

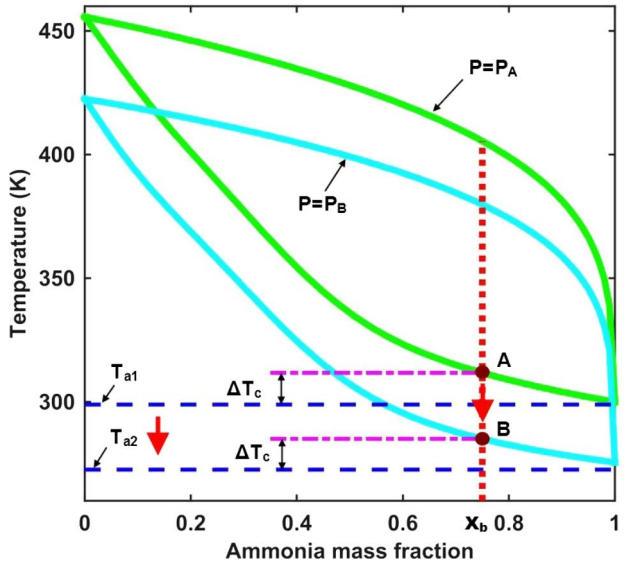

Fig. 3. Sliding condensation pressure method of the Kalina cycle as the ambient temperature varies.

2. Methodology

2.1. Kalina system with sliding condensation pressure

2.1.1. System description

In this study, a KSG-1 cycle is used to analysis the efficiency improvement using the sliding condensation pressure method for low-temperature geothermal power generation. The system schematic is shown in Fig. 1. The working fluid is a mixture of ammonia-water. The working processes are described as follows. The basic solution at the saturated liquid state 1 is pumped from the tank into the high-pressure path by the pump. The subcooled liquid at state 2 is heated to state 3 by the recuperator. Then, the basic solution absorbs the heat from the brine in the evaporator and transfers to the two-phase state 4. Because the heat source is a low-temperature geothermal brine at 120 ℃, the basic solution cannot be fully evaporated and a separator is employed to separate the two-phase fluid into an ammonia-rich saturated vapor mixture of state 5, which is also called the work solution, and an

Table 1
Input parameters for the Kalina system using sliding condensation pressure method.

Item	Parameter	Values
Heat source	Temperature T_{11}	120 ℃
	Mass flow rate $\dot{m}_{water}$	141.8 kg/s
	Pressure P_{11}	2 MPa
Evaporator	Minimal pinch $\Delta T_{e,PPTD}$	5 K
	Maximum output temperature T_4	107.3 ℃
	Maximum output pressure P_4	2.28 MPa
	Pressure drop (HT side) $\Delta P_{e,h}/P_{11}$	1.95%
	Pressure drop (LT side) $\Delta P_{e,l}/P_3$	1.94%
Recuperator	Minimal pinch $\Delta T_{re,PPTD}$	5 K
	Pressure drop (HT side) $\Delta P_{re,h}/P_9$	0.63%
	Pressure drop (LT side) $\Delta P_{re,l}/P_2$	2.8%
Condenser	Minimal pinch $\Delta T_{c,PPTD}$	10 K
	Pressure drop (HT side) $\Delta P_{c,h}/P_{10}$	1.93%
	Number of fans	40
	Power of fan	34 kW
	Air mass flow rate	120 kg/s per fan
Turbine	Isentropic efficiency η_t	0.85
	Maximum power	4 MW
Pump	Isentropic efficiency η_p	0.8
	Maximum power	200 kW

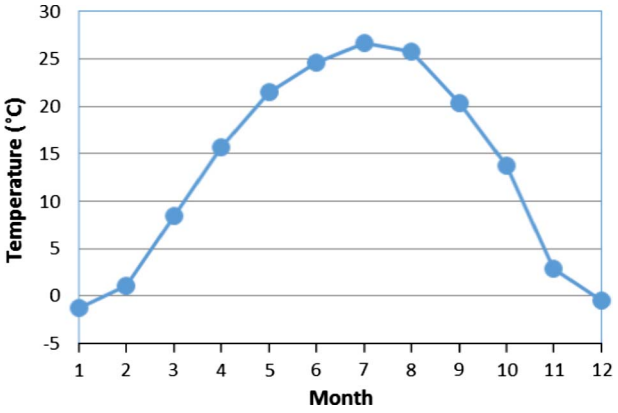

Fig. 4. Average monthly temperatures of a typical location with continental climates in Beijing (China).

ammonia-lean saturated liquid mixture of state 6. The high-pressure vapor mixture is expanded in the turbine whose expansion pressure ratio can be adjusted using sliding pressure control method and changed to state 7. On the other hand, the liquid mixture is throttled via the expansion valve to state 8. Subsequently, the low-pressure spent gas mixture is mixed with the low-pressure liquid flow in the mixer. The temperature of the two-phase fluid at state 9 drops after flowing through the recuperator. The basic solution at state 10 is fully condensed in the air-cooled condenser and turns back to the saturated liquid state 1. Fig. 2 shows the corresponding T-s and h-x diagrams of the working processes, where the relevant states are numbered and the dashed lines represent the bubble lines and the dotted lines denote the dew lines.

2.1.2. Working principle

An air-cooled condenser is used for the KSG-1 Kalina cycle system shown in Fig. 1. Normally, many Kalina cycle systems use water-cooled condensers. However, for some applications especially in an inland area, a large amount of water may be not available or too expensive [27]. Therefore, using air-cooled condensers is an alternative although this is vulnerable when the ambient temperature changes [28]. Previous research shows that tuning the composition of the ammonia-water mixture to match the changing ambient temperature can improve the average thermal efficiency of the KSG-1 Kalina cycle significantly [19]. In that method, the pressures at the inlet and outlet of the turbine remains constant and only the composition of ammonia-water mixture is adjusted as the ambient temperature varies.

In this study, a completely different method is investigated. The condensation pressure instead of the ammonia mass fraction is regulated according to the ambient temperature and its working principle is explained in Fig. 3. When the ambient temperature is T_{a1}, the basic working fluid (corresponding to State 1 in Fig. 1) is situated at State A. The temperature difference between State A and the ambient temperature is constrained by the pinch point temperature difference

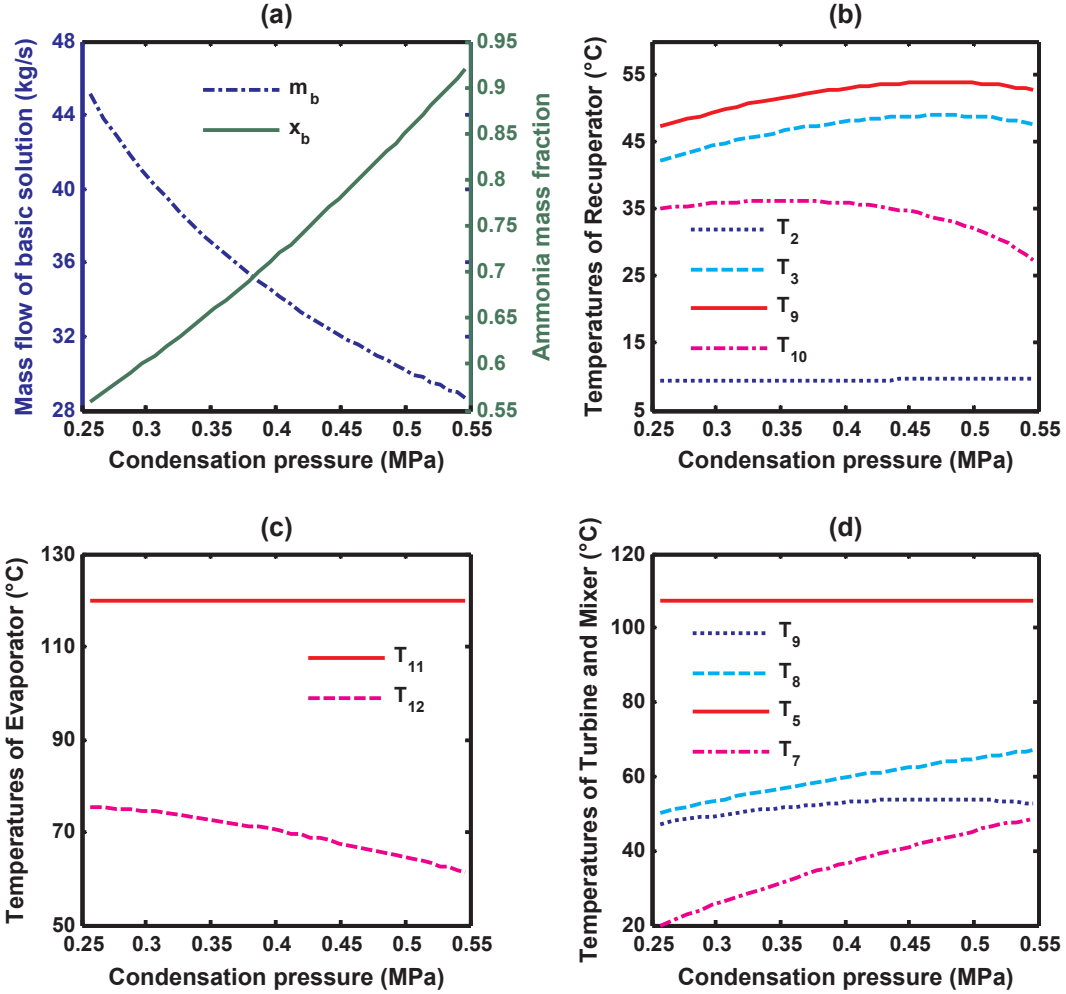

Fig. 5. System performance as a function of the condensation pressure for a fixed ambient temperature: (a) the mass flow rate and the ammonia mass fraction of the basic solution; (b) the temperatures at the inlet and outlet of the recuperator; (c) the temperatures of the geothermal brine; (d) the temperatures at the inlet and outlet of the turbine and the mixer.

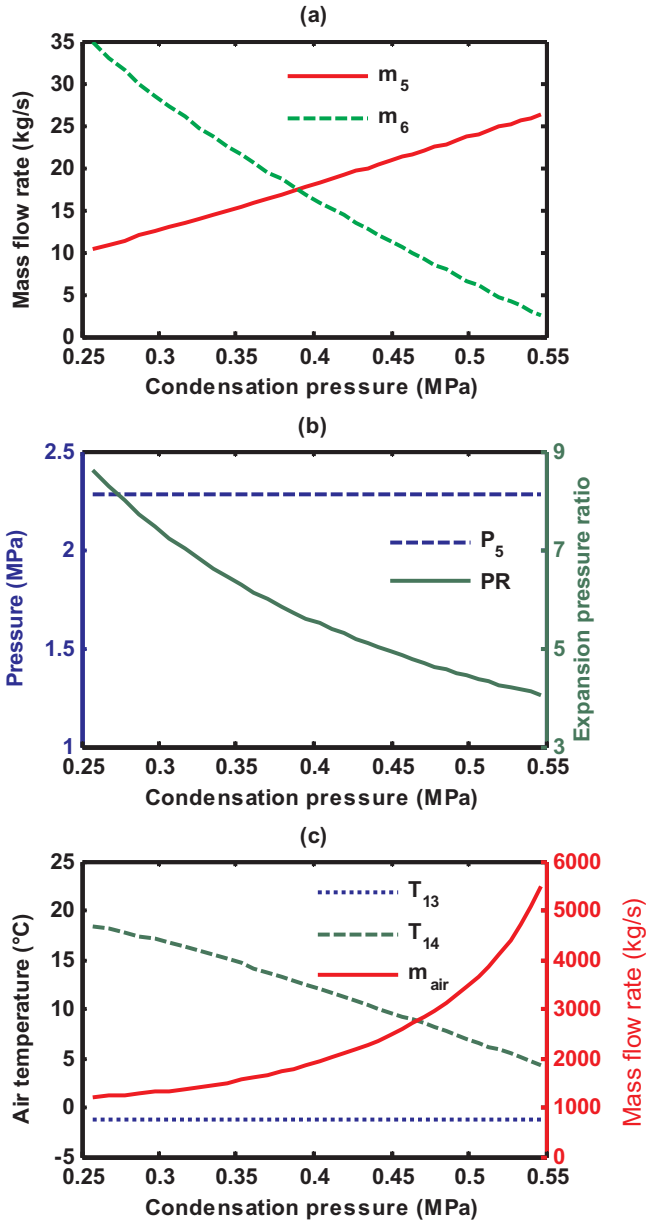

Fig. 6. System performance as a function of the condensation pressure under a fixed ambient temperature: (a) the mass flow rates at the outlets of the separator; (b) the expansion pressure ratio of the turbine; (c) the temperatures and the mass flow of the air.

(PPTD) of the condenser. The corresponding condensation pressure of State A is P_A. If the ambient temperature drops to T_{a2}, the condensation pressure can be decreased to P_B and the corresponding working state of the basic solution moves to State B. On the contrary, if the ambient temperature rises from T_{a2} to T_{a1}, the condensation pressure will increase accordingly from P_B to P_A. During the working process, the ammonia mass fraction is fixed and the temperature and pressure at the inlet of the turbine remains constant. The condensation pressure and the temperature at state 1 are adjusted via controlling the speed of the fans of the air-cooled condenser. Meanwhile, the expansion pressure ratio of the turbine and the mass flow rate of the working fluid are controlled by the speeds of the pump and the turbine, respectively.

2.2. Thermodynamic modeling

To analyze the efficiency improvement using the sliding condensation pressure method, a thermodynamic model based on the mass, energy, and exergy balance equations is developed and listed in the Appendix. In this model, all the working processes are assumed to be steady-state. The turbine is assumed to operate with a constant isentropic efficiency over the range of pressure ratios [29].

2.3. Numerical program development

A numerical program was developed using Matlab 2014 a and Refprop 9.1. The thermodynamic properties of ammonia-water mixture were computed by Refprop 9.1 based on the Helmholtz free energy method. The uncertainties for the equation of state are 0.2% in density, 2% in heat capacity, and 0.2% in vapor pressure [30]. In order to validate the accuracy of the program, the performance of a conventional KSG-1 cycle was computed first. The main input parameters for the program are given in Table 1. The results are compared with the data in Ref. [14] and the absolute errors for the heat transfer of the heat exchangers are less than 1.6%, which indicates the numerical program can be used to predict the performance of the Kalina cycle system.

The numerical program is then used to analyze the thermodynamic performance of the Kalina cycle with sliding condensation pressure. The data for Beijing, a typical continental climate [31] is used in this analysis and the air temperatures are shown in Fig. 4. The maximum ambient temperature can reach 26.6 °C in summer, while the minimum temperature can be low as −1.3 °C in winter.

The cycle performance is determined according to the average temperature of each month by the numerical program. The calculation processes are elaborated as follows. First, the temperature and mass flow rate of the geothermal brine are configured. The temperature and pressure at the outlet of the evaporator are also specified constantly and the operation pressures inside the system are calculated according to the relevant pressure drops listed in Table 1. Next, the temperature of the ammonia-water mixture at the inlet of the pump is computed according to the ambient temperature. Then, the corresponding condensation pressure is determined. In this analysis, the effect of the ammonia mass fraction on the system performance is also estimated. Therefore, an ammonia mass fraction of the basic solution needs to be assumed. According to the thermodynamic model in the Appendix, the operation process for each component of the Kalina cycle system is computed. Finally, the thermal and exergy efficiencies are obtained.

Based on the pinch point analysis, an iterative algorithm is developed to determine the heat transfer of the recuperator, the evaporator, and the condenser. Additionally, to avoid convergence problem close to the saturated lines of the ammonia-water mixture, the relative bubble and dew lines are determined at first and then the ammonia mass fractions at both the outlets of the separator are obtained according to the lever rule of zeotropic mixtures [32].

3. Results and discussion

3.1. Performance under a fixed ambient temperature

The system performance of the KSG-1 cycle at each month was evaluated by the numerical program. The results in January are used as a case study whose ambient temperature is fixed at −1.3 °C. The mass flow rate and the ammonia mass fraction of the basic solution as a function of the condensation pressure are shown in Fig. 5(a). The mass flow of the basic solution decreases from 45.17 kg/s to 28.70 kg/s when the condensation pressure increases from 0.257 to 0.547 MPa. The corresponding ammonia mass fraction increases from 0.56 to 0.92. Because the pinch point temperature difference in the condenser is constant, the temperature of the saturated liquid ammonia-water mixture at the outlet of the condenser is also fixed. Therefore, when the condensation pressure varies, the ammonia mass fraction of the basic solution must change accordingly. As a result, the specific heat capacity of the basic solution increases inside the evaporator, leading to a

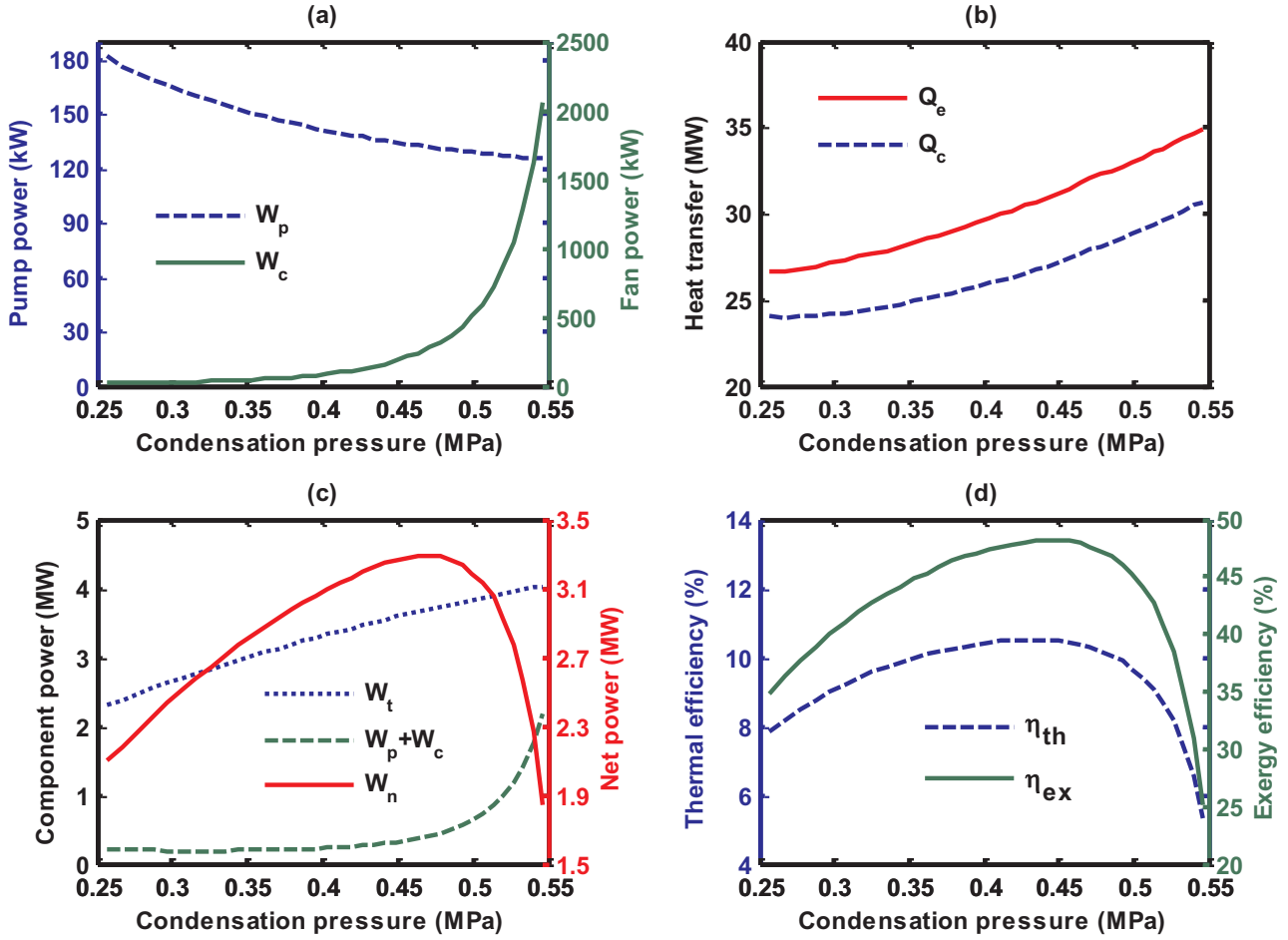

Fig. 7. System performance as a function of the condensation pressure for a fixed ambient temperature: (a) the power consumptions of the pump and the fans; (b) the heat transfer rates of the evaporator and the condenser; (c) the power output of the turbine and the net power of the Kalina cycle; (d) the thermal and exergy efficiencies.

Table 2
Thermodynamic properties of the Kalina cycle with the maximum thermal efficiency.

State	T (°C)	P (MPa)	h (kJ kg^{-1})	s (kJ kg^{-1} K^{-1})	$\dot{m}$ (kg s^{-1})	x (%)	Quality
1	9.20	0.435	130.1	1.105	32.673	0.760	0
2	9.56	2.392	133.4	1.107	32.673	0.760	0
3	48.62	2.325	332.6	1.767	32.673	0.760	0
4	107.3	2.28	1270.8	4.429	32.673	0.760	0.610
5	107.3	2.28	1823.4	6.005	19.914	0.964	1
6	107.3	2.28	408.38	1.970	12.759	0.441	0
7	39.80	0.447	1616.8	6.123	19.914	0.964	0.945
8	61.61	0.447	408.4	2.042	12.759	0.441	0.154
9	53.62	0.447	1144.9	4.534	32.673	0.760	0.628
10	35.14	0.443	945.7	3.909	32.673	0.760	0.541
11	120	2	505.1	1.526	141.8	–	–
12	68.63	1.961	288.9	0.937	141.8	–	–
13	−1.30	0.118	271.9	6.724	2259	–	–
14	10.45	0.113	283.8	6.779	2259	–	–

reduction of the mass flow rate. The temperatures at the inlet and outlet of the recuperator are given in Fig. 5(b). The temperatures of the brine are displayed in Fig. 5(c). The temperature of the brine at the outlet of the evaporator drops as the condensation pressure rises because of an easier evaporation of the basic solution. The temperatures in the turbine and the mixer are shown in Fig. 5(d).

The mass flow rates at the outlets of the separator are shown in Fig. 6(a). The mass flow of the work solution increases as the condensation pressure rises while the mass flow of the lean solution decreases due to an increment of the ammonia mass fraction of the basic solution. The pressure at the inlet of the turbine and the expansion pressure ratio are shown in Fig. 6(b). The temperatures and the mass flow of the air are shown in Fig. 6(c). The mass flow rate of the air increases significantly with an increment of the condensation pressure. Accordingly, the temperature of the air at the outlet reduces gradually.

The power consumptions of the Kalina cycle system are given in Fig. 7(a). The power input of the pump decreases gradually as the condensation pressure rises while the power input of the fans increase

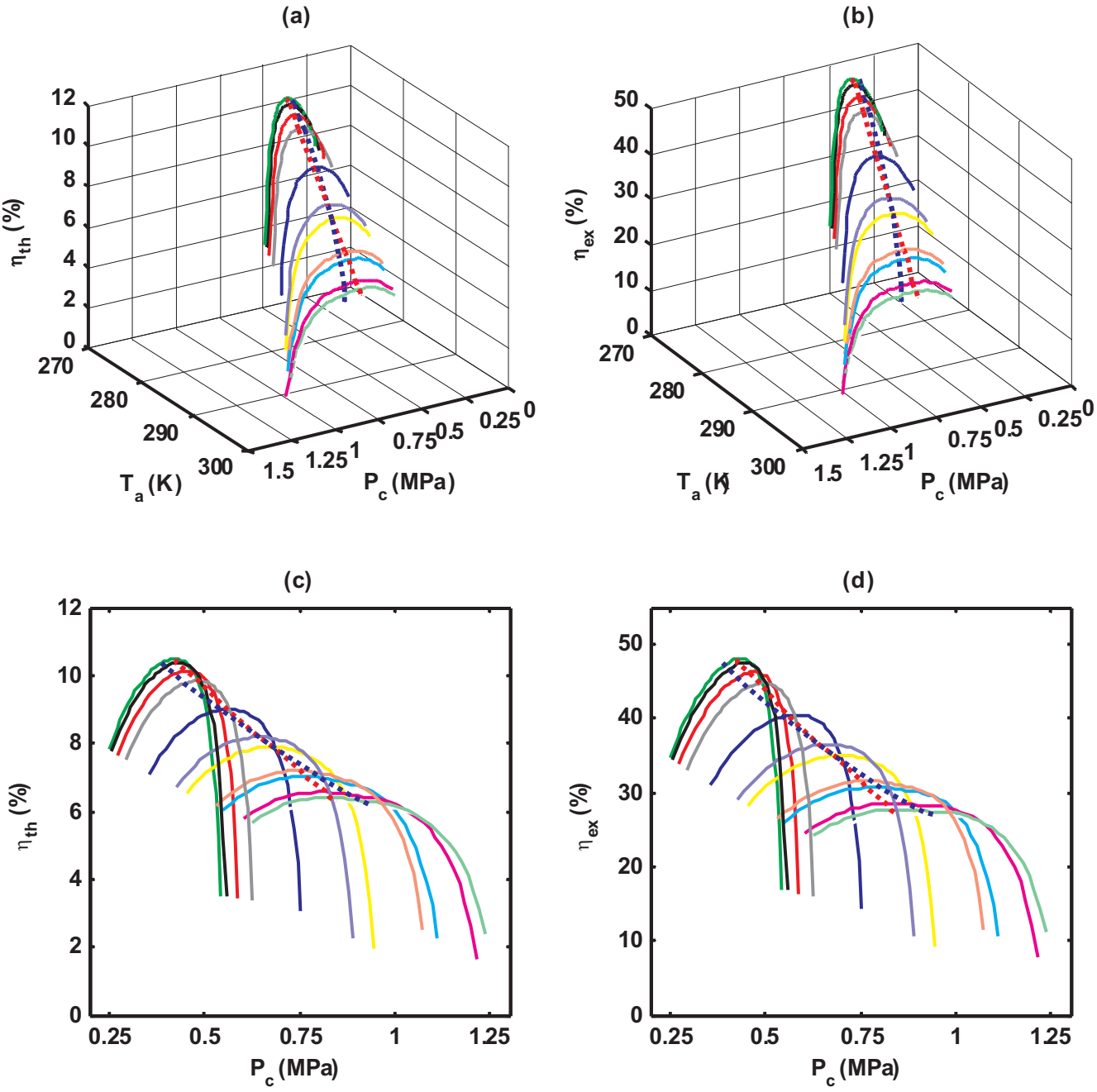

Fig. 8. Results of the Kalina cycle with sliding condensation pressure when the ambient temperature varies: (a) the thermal efficiency as a function of the ambient temperature and the condensation pressure; (b) the exergy efficiency as a function of the ambient temperature and the condensation pressure; (c) the thermal efficiency vs the condensation pressure; (d) the exergy efficiency vs the condensation pressure.

rapidly because the mass flow rate of the air rises significantly. The amounts of the heat transfer in the evaporator and the condenser are given in Fig. 7(b), respectively. Both are increased evidently. The power output of the turbine and the net power of the Kalina cycle system are displayed in Fig. 7(c). The power output of the turbine rises with an increment of the condensation pressure because of the augmentation of the mass flow rate of the work solution. The overall power consumption increases significantly if the condensation pressure is greater than 0.5 MPa. As a result, the net power output firstly increases and then decreases and there exists an optimal condensation pressure where the net power output is maximized.

The thermal and exergy efficiencies of the Kalina cycle system are given in Fig. 7(d). Both show a tendency of first increasing and then decreasing as the condensation pressure increases. It can be seen that the condensation pressure has a great influence on the system performance. The maximum value of the thermal efficiency is reached when the condensation pressure is 0.435 MPa. The thermodynamic properties of the KSG-1 Kalina cycle when the thermal efficiency is maximized are listed in Table 2. The corresponding maximal thermal efficiency is 10.48% and the exergy efficiency is 48.10%.

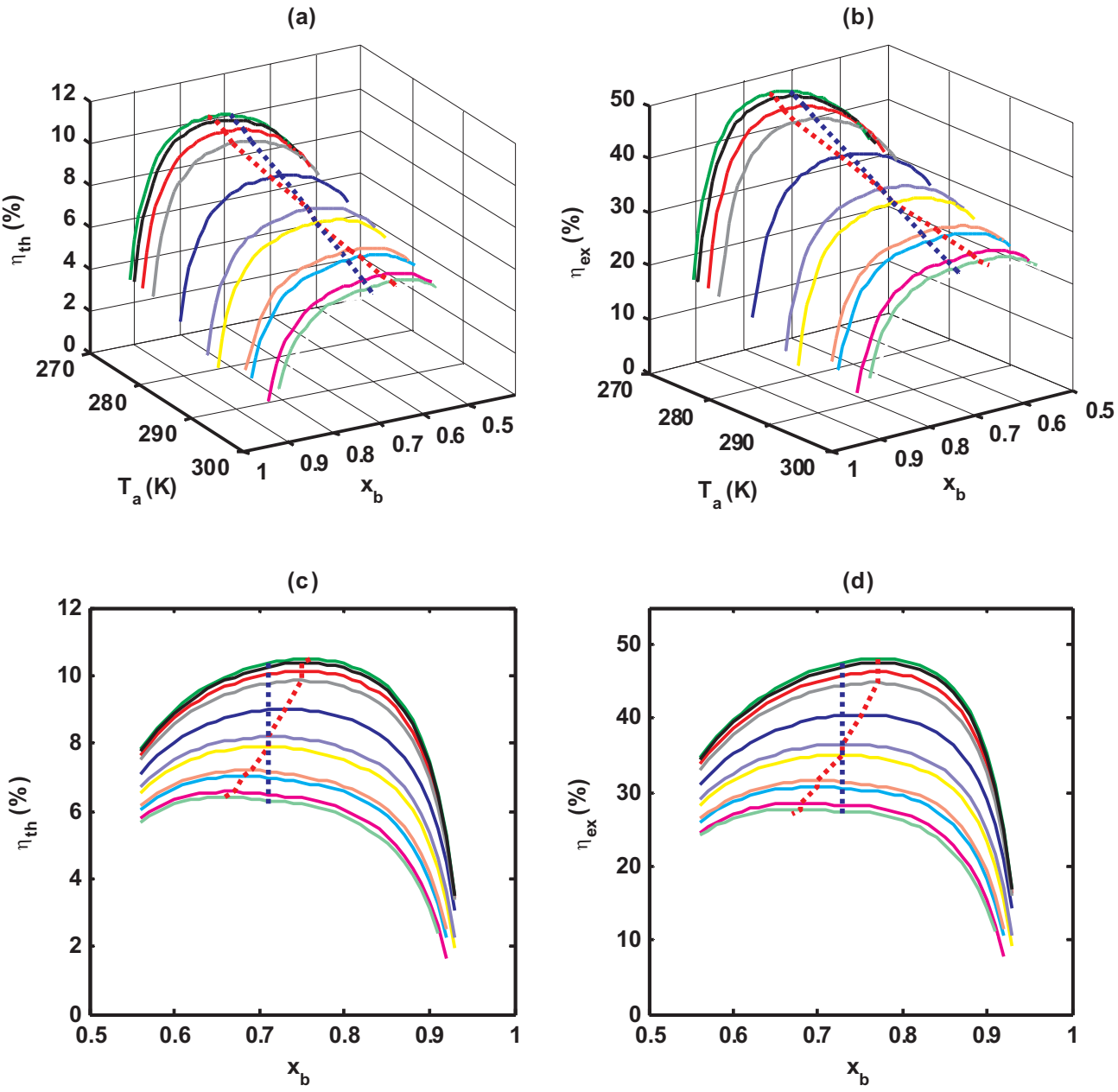

Fig. 9. Results of the Kalina cycle with sliding condensation pressure when the ambient temperature varies: (a) the thermal efficiency as a function of the ambient temperature and the ammonia mass fraction; (b) the exergy efficiency as a function of the ambient temperature and the ammonia mass fraction; (c) the thermal efficiency vs the ammonia mass fraction; (d) the exergy efficiency vs the ammonia mass fraction.

3.2. Performance with sliding condensation pressure

Based on the ambient temperature given in Fig. 4, the system performance as a function of the condensation pressure at each month is analyzed. Accordingly, the optimal condensation pressure under each ambient temperature can be determined.

Fig. 8(a) and (b) show the thermal and exergy efficiencies of the KSG-1 cycle as a function of the ambient temperature and the condensation pressure. For a fixed ambient temperature, the thermal and exergy efficiencies first increase and then decrease as the condensation pressure increases. There exists an optimal point where the thermal efficiency is maximized. On the other hand, the system efficiency increases evidently as the ambient temperature drops. The corresponding optimal point shifts from high condensation pressure to low condensation pressure. In these figures, the red dashed line shows the optimal trajectory of the thermal efficiency and the blue dashed line denotes the results of a fixed ammonia mass fraction of 0.71. The optimized results of x_b based on the thermal efficiency are in the range of 0.66–0.76, whose average value is around 0.71. This average value is used for the Kalina cycle with sliding condensation pressure. The corresponding thermal and exergy efficiencies as a function of the condensation pressure are shown in Fig. 8(c) and (d), respectively. It can be seen that the allowable range of the condensation pressure narrows as the ambient temperature drops. In summer, the range of the

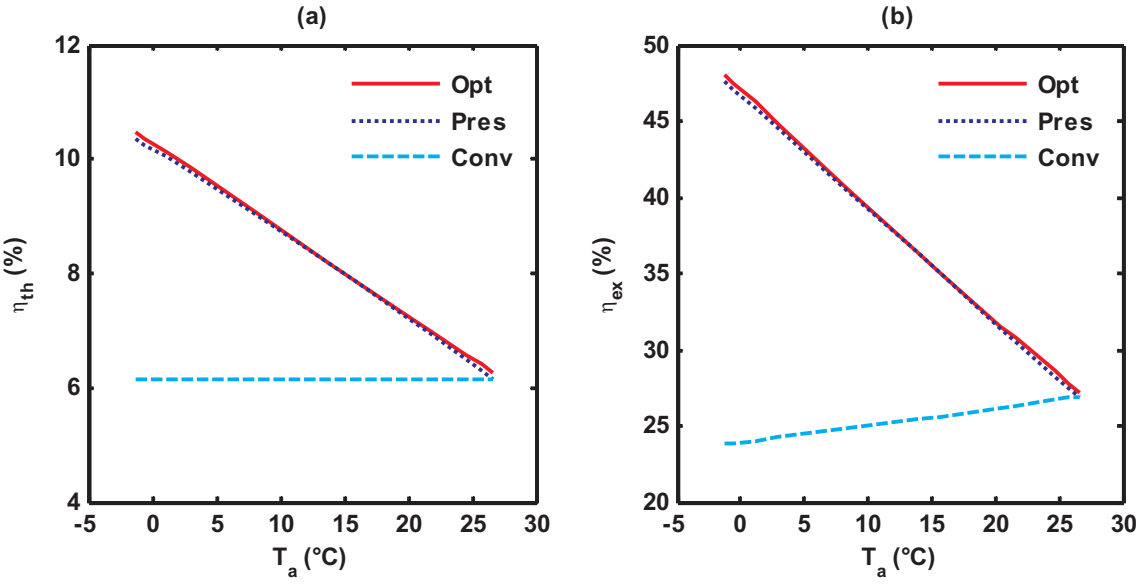

Fig. 10. Efficiency comparison of the Kalina cycles: (a) the thermal efficiency; (b) the exergy efficiency. (Conv represents the conventional Kalina cycle; Press denotes the Kalina cycle with sliding condensation pressure; Opt is the Kalina cycle operating along with the optimal trajectory.)

Table 3
Performance improvements of the Kalina cycle with sliding condensation pressure.

Cycles	W_n (MW)	Q_e (MW)	η_{th} (%)	α	β	γ
Conv	1.534	24.93	6.15			
Press	2.251	27.10	8.21	46.72	8.72	33.50
Opt	2.282	27.09	8.28	48.76	8.70	34.63

Conv: the conventional Kalina cycle.
Press: the Kalina cycle with sliding condensation pressure.
Opt: the Kalina cycle operating along the optimal trajectory.

condensation pressure is large and the intervals with a high efficiency is big. However, in winter, the allowable range of the condensation pressure reduces to almost the half and the corresponding intervals with a high efficiency become very small. This characteristic will increase the difficulty of the condensation pressure control in winter.

From the results of Fig. 8, the ammonia mass fraction of the optimal trajectory is not constant. However, this parameter is assumed to be fixed for the Kalina cycle with sliding condensation pressure. Therefore, it is important to study how to specify the ammonia mass fraction of the Kalina cycle with sliding condensation pressure. From the results of the above section, it can be seen that the condensation pressure has a bijective relationship with the ammonia mass fraction. Therefore, the results in Fig. 8 also can be plotted as a function of the ambient temperature and the ammonia mass fraction shown as Fig. 9. The corresponding optimal trajectory and the results for the sliding condensation pressure method with a fixed ammonia mass fraction of 0.71 are also shown in these figures. It can be seen that the allowable ranges of the ammonia mass fraction for all the ambient temperature are almost the same as 0.5–0.91. Furthermore, the high-efficiency interval of the ammonia mass fraction for each ambient temperature is very large, which means that the ammonia mass fraction is not as sensitive as the condensation pressure. It is evident that the efficiency with a fixed ammonia mass fraction of 0.71 is close to that of the optimal trajectory. To give a clear comparison, the thermal and exergy efficiencies of the three Kalina cycles as a function of the ambient temperature are shown in Fig. 10. The efficiency of the Kalina cycle with sliding condensation pressure is very close to the optimal results. The lower dashed lines represent the results of the corresponding conventional Kalina cycle. It can be found that the energy efficiency of the Kalina cycle with sliding condensation pressure can be very close to that of the optimal results and can be improved significantly compared with the conventional Kalina cycle as the ambient temperature decreases.

The annual average efficiency improvement of the Kalina cycle with sliding condensation pressure is very close to the optimal results listed in Table 3. The evaluated average thermal efficiency of the Kalina cycle with sliding condensation pressure can achieve 8.21%, improved by 33.5% compared with the conventional Kalina cycle.

The reason for such a great efficiency improvement can be explained by Fig. 11. As the ambient temperature decreases, the net power output of the Kalina cycle with sliding condensation pressure increases evidently shown in Fig. 11(a). This increment is mainly because of the decrease of the condensation pressure shown in Fig. 11(b). The pressure at the inlet of the turbine is constant. Thus, the expansion pressure ratio of turbine increases gradually as the ambient temperature drops shown in Fig. 11(c).

The evaluated air mass flow rate is 1856 kg/s when the ambient temperature is −1.3 °C while it decreases to 1566 kg/s when the ambient temperature increases to 26.6 °C. Normally, the mass flow of the fan has a linear relationship with the fan speed. If the rated speed of the fans of the air-cooled condenser is 900 r/min, the fan speed will decrease from 900 to 760 r/min as the ambient temperature rises from −1.3 to 26.6 °C. Generally, the variation time of the ambient temperature is of the order of hours. However, studies indicated that the transient response time of a Kalina cycle normally was less than 20 min [33]. In practice, the speed of the fans can be regulated to the target speed in a few seconds. Therefore, the speed of the fans can be controlled to follow the variation of the ambient temperature. On the other hand, the working fluid temperature at the outlet of the condenser can be regulated with the ambient temperature by the speed of the fans. To keep the relative condensation pressure sliding with the ambient temperature, the expansion pressure ratio of the turbine must be regulated as in Fig. 11(c) by controlling the speed of the turbine. Because the expansion pressure ratio is regulated according to the variation of the ambient temperature and the speed of the turbine can be tuned in a few minutes, this method can satisfy the requirement of the response time. The detailed investigation of the transient performance of the Kalina

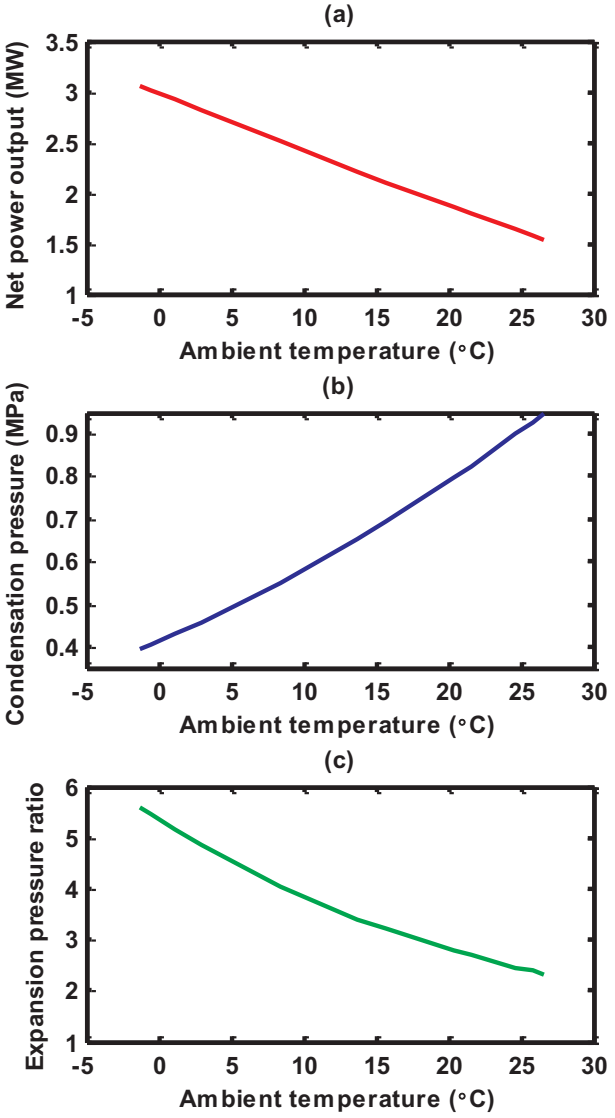

Fig. 11. Results of the Kalina cycle with sliding condensation pressure as a function of the ambient temperature: (a) the net power output; (b) the condensation pressure; (c) the expansion pressure ratio.

cycle with sliding condensation pressure method and the effect of different control algorithms are beyond the scope of this paper due to the page limitation.

3.3. Comparison with the composition tuning method

A previous investigation indicated that using a composition tuning method could improve the efficiency of Kalina cycle significantly when the ambient temperature varies [19]. In this section, the efficiency improvement of sliding condensation pressure is compared with the composition tuning method. The results are shown in Fig. 12.

The boundary conditions for the three Kalina cycles are the same and the net power outputs are shown in Fig. 12(a). It can be seen that the net power output of the Kalina cycle with sliding condensation pressure is almost the same with that of the composition-adjustable Kalina cycle. Both are higher than that of the conventional Kalina cycle.

For the composition-adjustable Kalina cycle, the condensation pressure stays constant and only the ammonia mass fraction is tuned when the ambient temperature drops. In this way, the enthalpy difference of the ammonia-water mixture between the inlet and outlet of the turbine increases, leading to an increase of the net power output as the ambient temperature decreases. However, for the Kalina cycle with sliding condensation pressure, the ammonia mass fraction is fixed and only the condensation pressure is adjusted according to the ambient temperature. Using this method, the pressure expansion ratio of the turbine increases as the ambient temperature drops, leading to an improvement of the net power output. Either the sliding condensation pressure method or the composition tuning method can adjust the condensation temperature at the outlet of the condenser to 10 °C higher than the ambient temperature. Therefore, their net power outputs are very close.

The thermal efficiencies of the three cycles are shown in Fig. 12(b). It can be seen that the thermal efficiency of the Kalina cycle with sliding condensation pressure is almost the same as the composition-adjustable Kalina cycle when the ambient temperature is above 15 °C. However, as the ambient temperature drops further, the thermal efficiency of the Kalina cycle with sliding condensation pressure is higher than that of the composition-adjustable Kalina cycle because more heat is absorbed in the evaporator for the composition-adjustable Kalina.

Table 4 compares the annual average thermal efficiencies of the three Kalina cycles. It can be seen the annual average thermal efficiency of the Kalina cycle with sliding condensation pressure can be improved by 33.5% compared with the conventional Kalina cycle while the efficiency improvement of the composition-adjustable Kalina cycle is only 27.8%.

4. Conclusions

This paper investigates the efficiency improvement of a Kalina cycle with sliding condensation pressure method. An analysis program has been developed based on the system's thermodynamic model. The operation characteristics and energy efficiency with the adjustment of the condensation pressure are estimated as the ambient temperature varies over a year. The obtained results are compared to the conventional Kalina cycle and the composition-adjustable Kalina cycle. The main conclusions are summarized as follows:

(1) For low-temperature geothermal power generation, the Kalina cycle with sliding condensation pressure method can adjust the condensation temperature to match the ambient temperature. In this way, the expansion pressure ratios of the turbine and the net power output can be improved significantly and the exergy destruction in the condenser can be decreased when the ambient temperature drops. Although the ammonia mass fraction is not as sensitive as the condensation pressure for the Kalina cycle with sliding condensation pressure, it must be selected within an appropriate range using the presented procedures.
(2) Further adjustment of the ammonia mass fraction of the Kalina cycle with sliding condensation pressure can only improve the efficiency slightly. The reason is that the exergy destruction rate in the condenser has already been decreased significantly with sliding condensation pressure method.
(3) The annual average efficiency of the Kalina cycle with sliding condensation pressure is better than the composition-adjustable Kalina cycle. Meanwhile, the composition-adjustable Kalina cycle keeps the condensation pressure constant during its working process, resulting in a limited allowable range of the ambient temperature. If the ambient temperature drops too low or too high, the composition-adjustable Kalina cycle cannot guarantee a good

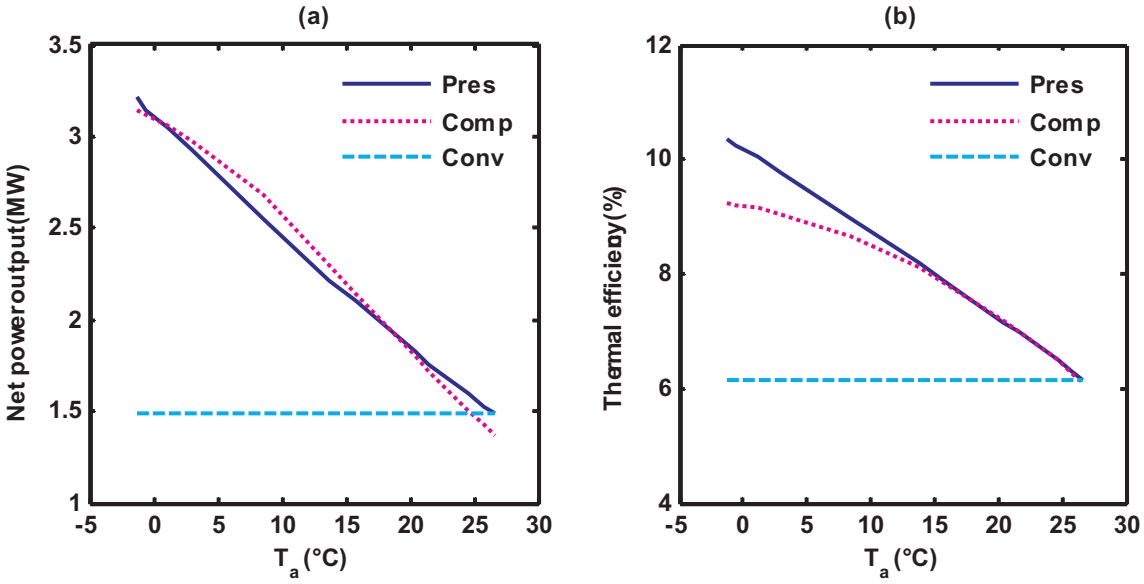

Fig. 12. Efficiency comparison between the Kalina cycle with sliding condensation pressure and the composition-adjustable Kalina cycle: (a) the net power output; (b) the thermal efficiency. (Conv represents the conventional Kalina cycle; Press denotes the Kalina cycle with sliding condensation pressure; Comp is the composition-adjustable Kalina cycle.)

Table 4
Comparison between the Kalina cycle with sliding condensation pressure and the composition-adjustable Kalina cycle.

Cycles	W_n (MW)	Q_e (MW)	η_{th} (%)	α	β	γ
Conv	1.534	24.93	6.15			
Press	2.251	27.10	8.21	46.72	8.72	33.5
Comp	2.267	28.21	7.86	47.78	13.16	27.8

Conv: the conventional Kalina cycle.
Press: the Kalina cycle with sliding condensation pressure.
Comp: the composition-adjustable Kalina cycle.

temperature match in the air-cooled condenser. Under these ambient conditions, the sliding condensation pressure method has an advantage over the composition tuning method. Therefore, compared with the composition tuning method, the sliding condensation pressure method is another good way to improve the energy efficiency of the Kalina cycle.

Acknowledgements

This research is funded by EPSRC (Ref: EP/N005228/1 and EP/N020472/1) and Royal Society (Ref: IE150866) in the UK.

Appendix A

To analyze the energy efficiency of the Kalina cycle system with sliding condensation pressure, a thermodynamic model based on the mass, energy, and exergy balance equations is developed.

The pump:

$$\dot{W}_p = \dot{m}_1(h_2 - h_1) = \dot{m}_1(h_{2,s} - h_1)/\eta_p \quad \text{(A1)}$$

$$\dot{I}_p = \dot{E}_1 - \dot{E}_2 + \dot{W}_p \quad \text{(A2)}$$

where E_i is the exergy of state i and I_p is the exergy destruction rate of the pump.

The recuperator:

$$\dot{Q}_{re} = \dot{m}_2(h_3 - h_2) = \dot{m}_9(h_9 - h_{10}) \quad \text{(A3)}$$

$$\dot{I}_{re} = \dot{E}_2 - \dot{E}_3 + \dot{E}_9 - \dot{E}_{10} \quad \text{(A4)}$$

The evaporator:

$$\dot{Q}_e = \dot{m}_3(h_4 - h_3) = \dot{m}_{water}(h_{11} - h_{12}) \quad \text{(A5)}$$

$$\dot{I}_e = \dot{E}_3 - \dot{E}_4 + \dot{E}_{11} - \dot{E}_{12} \quad \text{(A6)}$$

The separator:

$$\dot{m}_4 x_4 = \dot{m}_5 x_5 + \dot{m}_6 x_6 \quad \text{(A7)}$$

$$\dot{m}_4 = \dot{m}_5 + \dot{m}_6 \quad \text{(A8)}$$

$$\dot{m}_4 h_4 = \dot{m}_5 h_5 + \dot{m}_6 h_6 \quad \text{(A9)}$$

$$r = \frac{x_4 - x_6}{x_5 - x_6} \tag{A10}$$

$$\dot{I}_s = \dot{E}_4 - \dot{E}_5 - \dot{E}_6 \tag{A11}$$

where x_i is the ammonia mass fraction at state i and r is the mass ratio of the ammonia-rich vapor of state 5 to the basic solution of state 4.

The turbines:

$$\dot{W}_t = \dot{m}_5(h_5 - h_7) = \dot{m}_5(h_5 - h_{7,s})\eta_t \tag{A12}$$

$$PR = P_5/P_7 \tag{A13}$$

$$\dot{I}_t = \dot{E}_5 - \dot{E}_7 - \dot{W}_t \tag{A14}$$

The expansion valve:

$$h_8 = h_6 \tag{A15}$$

$$\dot{I}_v = \dot{E}_6 - \dot{E}_8 \tag{A16}$$

The mixer:

$$\dot{m}_9 x_9 = \dot{m}_7 x_7 + \dot{m}_8 x_8 \tag{A17}$$

$$\dot{m}_9 = \dot{m}_7 + \dot{m}_8 \tag{A18}$$

$$\dot{m}_9 h_9 = \dot{m}_7 h_7 + \dot{m}_8 h_8 \tag{A19}$$

$$\dot{I}_m = \dot{E}_7 + \dot{E}_8 - \dot{E}_9 \tag{A20}$$

The air-cooled condenser:

$$\dot{Q}_c = \dot{m}_{10}(h_{10} - h_1) = \dot{m}_{air}(h_{14} - h_{13}) \tag{A21}$$

$$\dot{I}_c = \dot{E}_{17} - \dot{E}_1 + \dot{W}_c \tag{A22}$$

The power input of the fans of the air-cooled condenser is calculated by [34]

$$\dot{W}_c = N_f \dot{W}_{f0}\left(\frac{\dot{m}_f}{\dot{m}_{f0}}\right)^3 \tag{A23}$$

$$\dot{m}_f = \dot{m}_{air}/N_f \tag{A24}$$

where N_f is the number of the fans, $\dot{m}_f$, $\dot{m}_{f0}$ are the actual and rated fan air mass flow rates, and $\dot{W}_{f0}$ is the rated fan power input.

The net power output of the Kalina cycle system is

$$\dot{W}_n = \dot{W}_t - \dot{W}_{p1} - \dot{W}_{p2} - \dot{W}_c \tag{A25}$$

The thermal efficiency of the Kalina cycle is defined as

$$\eta_{th} = \dot{W}_n/\dot{Q}_e \tag{A26}$$

The exergy efficiency of the Kalina cycle is

$$\eta_{ex} = \frac{\dot{W}_n}{\dot{E}_{11} - \dot{E}_{12}} \tag{A27}$$

The annual average performance indexes including the net power output, the heat transfer from the heat source, and the thermal efficiency for the Kalina cycle are calculated using equations (A28), (A29), and (A30), respectively.

$$\overline{W}_n = \frac{1}{N}\sum_{i=1}^{N} \dot{W}_n(i), \tag{A28}$$

$$\overline{Q}_e = \frac{1}{N}\sum_{i=1}^{N} \dot{Q}_e(i), \tag{A29}$$

$$\overline{\eta}_{th} = \frac{1}{N}\sum_{i=1}^{N} \eta_{th}(i), \tag{A30}$$

where N is the total months of a year.

The annual average improvements of the Kalina cycle with sliding condensation pressure relative to the conventional Kalina cycle are determined by

$$\alpha = \frac{\overline{W}_{n,press} - \overline{W}_{n,conv}}{\overline{W}_{n,conv}} \times 100\%, \tag{A31}$$

$$\beta = \frac{\overline{Q}_{e,press} - \overline{Q}_{e,conv}}{\overline{Q}_{e,conv}} \times 100\%, \tag{A32}$$

$$\gamma = \frac{\overline{\eta}_{th,press} - \overline{\eta}_{th,conv}}{\overline{\eta}_{th,conv}} \times 100\%. \quad \text{(A33)}$$

References

[1] Li K, Liu C, Chen Y, Liu G, Chen J. Upgrading both geothermal and solar energy. In: Proceedings of 41st Workshop on Geothermal Reservoir Engineering. Stanford University, California, USA; 22–24 February 2016.

[2] Chamorro CR, Garcia-Cuesta JL, Mondejar ME, Perez-Madrazo A. Enhanced geothermal systems in Europe: an estimation and comparison of the technical and sustainable potentials. Energy 2014;65:250–63.

[3] Bertani R. Geothermal power generation in the world 2010–2014 update report. Geothermics 2016;60:31–43.

[4] Zhang X, He M, Zhang Y. A review of research on the Kalina cycle. Renew Sustain Energy Rev 2012;16:5309–18.

[5] Modi A, Haglind F. A review of recent research on the use of zeotropic mixtures in power generation systems. Energy Convers Manage 2017;138:603–26.

[6] Hua J, Chen Y, Wu J. Thermal performance of a modified ammonia-water power cycle for reclaiming mid/low-grade waste heat. Energy Convers Manage 2014;85:453–9.

[7] Pradeep Varmaa GV, Srinivas T. Power generation from low temperature heat recovery. Renew Sustain Energy Rev 2017;75:402–14.

[8] Fallah M, Mahmoudi SMS, Yari M, Ghiasi RA. Advanced exergy analysis of the Kalina cycle applied for low temperature enhanced geothermal system. Energy Convers Manage 2016;108:190–201.

[9] Ma Z, Bao H, Roskilly AP. Principle investigation on advanced absorption power generation cycles. Energy Convers Manage 2017. http://dx.doi.org/10.1016/j.enconman.2017.02.078.

[10] Kalina AI, Pelletier RI, Rhodes LB. Method and apparatus of converting heat to useful energy. US patent 5953918; 1999.

[11] Mlcak H, Mirolli M, Hjartarson H, Ralph M. Notes from the north: a report on the debut year of the 2 MW Kalina cycle geothermal power plant in Husavik, Iceland. In: Geothermal Resources Council 2002 Annual Meeting. Reno, Nevada, USA; 22–25 September 2002.

[12] Saffari H, Sadeghi S, Khoshzat M, Mehregan P. Thermodynamic analysis and optimization of a geothermal Kalina cycle system using Artificial Bee Colony algorithm. Renew Energy 2016;89:154–67.

[13] Arslan O. Power generation from medium temperature geothermal resources: ANN-based optimization of Kalina cycle system-34. Energy 2011;36:2528–34.

[14] Lengert J. Method and device for carrying out a thermodynamic cyclic process. US patent 2007/0022753; 2007.

[15] Mergner H, Weimer T. Performance of ammonia-water based cycles for power generation from low enthalpy heat sources. Energy 2015;88:93–100.

[16] Ibrahim MB, Kovach RM. A Kalina cycle application for power generation. Energy 1993;18:961–9.

[17] Nguyen TV, Knudsen T, Larsen U, Haglind F. Thermodynamic evaluation of the Kalina split-cycle concepts for waste heat recovery applications. Energy 2014;71:277–88.

[18] Mlcak HA, Mirolli MD. System and methods for increasing the efficiency of a Kalina cycle. US patent 8744636; 2014.

[19] Wang E, Yu Z. A numerical analysis of a composition-adjustable Kalina cycle power plant for power generation from low-temperature geothermal sources. Appl Energy 2016;180:834–48.

[20] Aanstad OJ. Method and apparatus for controlling a steam turbine. US patent 4005581; 1977.

[21] Silvestri J, George J. Method for heat rate improvement in partial-arc steam turbine. US patent 4888954; 1989.

[22] Jonshagen K, Genrup M. Improved load control for a steam cycle combined heat and power plant. Energy 2010;35:1694–700.

[23] Hu D, Zheng Y, Wu Y, Li S, Dai Y. Off-design performance comparison of an organic Rankine cycle under different control strategies. Appl Energy 2015;156:268–79.

[24] Usman M, Imran M, Lee DH, Park BS. Experimental investigation of off-grid organic Rankine cycle control system adapting sliding pressure strategy under proportional integral with feed-forward and compensator. Appl Therm Eng 2017;110:1153–63.

[25] Modi A, Andreasen JG, Karn MR, Haglind F. Part-load performance of a high temperature Kalina cycle. Energy Convers Manage 2015;105:453–61.

[26] Li H, Hu D, Wang M, Dai Y. Off-design performance analysis of Kalina cycle for low temperature geothermal source. Appl Therm Eng 2016;107:728–37.

[27] Walraven D, Laenen B, D'haeseleer W. Minimizing the levelized cost of electricity production from low-temperature geothermal heat sources with ORCs: water or air cooled? Appl Energy 2015;142:144–53.

[28] Collings P, Yu Z, Wang E. A dynamic organic Rankine cycle using a zeotropic mixture as the working fluid with composition tuning to match changing ambient conditions. Appl Energy 2016;171:581–91.

[29] Pierobon L, Nguyen TV, Mazzucco A, Larsen U, Haglind F. Part-load performance of a wet indirectly-fired gas turbine integrated with an Organic Rankine Cycle turbogenerator. Energies 2014;7(12):8294–316.

[30] Lemmon EW, Huber ML, McLinden MO. NIST standard reference database 23: reference fluid thermodynamic and transport properties-REFPROP, version 9.1. Gaithersburg: National Institute of Standards and Technology, Standard Reference Data Program; 2013.

[31] TuTiempo.net. Global climate data; 2015. < http://lishi.tianqi.com/beijing/index.html>.

[32] Walas SM. Phase equilibria in chemical engineering. Boston: Butterworth Publishers; 1984.

[33] Hua J, Chen Y, Wu J, Zhi Z, Dong C. Waste heat supply-side power regulation with variable concentration for turbine in Kalina cycle. Appl Therm Eng 2015;91:583–90.

[34] Sun J, Li W. Operation optimization of an organic rankine cycle (ORC) heat recovery power plant. Appl Therm Eng 2011;31:2032–41.